

# A complete mean-field theory for dynamics of binary recurrent neural networks

Farzad Farkhooi<sup>a,b,1</sup> and Wilhelm Stannat<sup>a,b</sup>

<sup>a</sup>Institut für Mathematik, Technische Universität Berlin, D-10623 Berlin, Germany.

<sup>b</sup>Bernstein Center for Computational Neuroscience, D-10115 Berlin, Germany.

<sup>1</sup>farzad@bccn-berlin.de

March 10, 2022

## Abstract

Recurrent networks of binary units provide a prototype for complex interactions in neuronal networks. In the theoretical analysis of their collective dynamics, it is often assumed that unit interactions in the network are homogeneous. Here, we derive a unified theory that encompasses the macroscopic dynamics of recurrent networks with arbitrary connectivity architectures. We identify conditions to the connectivity patterns for which the population averages, according to mean-field theory, converge to a deterministic limit as the size of the system increases. The mathematical analysis, using the martingale structure of the network's Markovian dynamics, further quantifies the aggregate fluctuation of the population activity in a finite-size system. Our theory allows, without additional effort, the investigation of systems that do not exhibit a pointwise convergence to the mean-field limit. In particular, we uncover a novel dynamic state in which a system with inhomogeneous micro-structures in the network connectivity, along with an asynchronous behavior, also exhibits stochastic synchronization. This phenomenon resembles non-trivial fluctuations in the average population activity, which can survive irrespective of system size. The concise mathematical analysis that is presented here enables formulation of mean-field equation for these cases in the form of a stochastic ordinary differential equation. Our results indicate the essential elements for implementation of connectivity motifs in the general theory of recurrent networks.

# 1 Introduction

The fundamental characteristics of collective spiking dynamics in neural systems remain elusive. For instance, it is a challenge to consistently explain experimental data that exhibit wide modes of complex macroscopic dynamics, ranging from a variety of synchronous to asynchronous states, in cortical circuitry [13, 14, 16, 10, 11]. The prevailing theoretical models, so-called balanced networks, exhibit self-generated fluctuations [18, 12, 6] that successfully explain the irregular asynchronous state that has been observed in the cortical spiking activity. The description of the asynchronous state is closely related to the formulation of a mean-field theory (MFT) that replaces the statistics of individual units with population averages; this is similar to the statistical mechanics of spin glasses [5] in the thermodynamic limit. In the analysis of the balanced state, the number of units in the network,  $N$ , is assumed to be large (i.e.  $N \rightarrow \infty$ ) and the average number of direct interactions per unit,  $K$ , is assumed to be substantial and homogeneous (i.e.  $K \rightarrow \infty$ ). To date, no theory has been developed for finite-size corrections with respect to realistic values of  $N$  and  $K$ . Additionally, a growing body of experimental evidence is emerging [15, 7, 9] that contradicts the assumptions that the network architecture follows a homogeneous and uniformly random Bernoulli directed graph (directed Erdős-Rényi network) that is commonly used in the classical analysis of cortical models [18, 12, 6]. It is not yet understood how the combination of these realistic connectivity micro-structures and the finite-size of biological networks influence the modes of the network dynamics. Therefore, it is important to determine whether the existence of these inhomogeneous structures in the architecture of connectivity is able to alter the MFT predictions for cortical networks behavior. Understanding the various spiking dynamic states that can emerge within these realistic cortical networks has important implications for elucidating the temporal components of neuronal coding. Here, we develop a mathematical theory to determine the collective dynamics of a finite-sized neuronal population. We first develop a general MFT for binary units that interact within an arbitrary network architecture. To simplify our computations, we demonstrate our general method for connectivity matrices that have a fixed row sum, i.e., a fixed number  $K$  of inputs to units. Interestingly, we identify the conditions on the connectivity structure that are necessary to guarantee the convergence of the average population activity to a deterministic limit as  $N \rightarrow \infty$ . We show that whenever these conditions are satisfied, the classical results can be recovered in the thermodynamic limit. Using the martingale structure of the Markovian dynamics of the network, we compute the finite size effect and derive a corresponding dynamical equation in terms of an Ornstein-Uhlenbeck process. Furthermore, our approach reveals a novel dynamical state in a network with inhomogeneous coupling, in which the fluctuations of the average population activity survive irrespective of the network size. In this polychronous state [8], precise time-locked population events are able to emerge, whereas the overall network activity remains asynchronous.

## 2 Mean-field theory (MFT) for binary recurrent network

Consider a network that is described by an adjacency matrix  $\mathbf{J} = (J_{ij})$  of  $N$  binary units, whose their current states are denoted as  $\mathbf{n}(t) := (n_1(t), \dots, n_N(t))$ . The vector  $\mathbf{n}(t)$  is a time-continuous Markov chain on  $\{0, 1\}^N$  with  $Q$ -matrix, where  $Q(\mathbf{n}, \mathbf{m}) = 0$  if and only if  $\|\mathbf{n} - \mathbf{m}\| \geq 2$  and

$$Q(\mathbf{n}, \mathbf{m}) = \begin{cases} f_i(\mathbf{n}) & \text{if } \mathbf{m} - \mathbf{n} = e_i \\ 1 - f_i(\mathbf{n}) & \text{if } \mathbf{m} - \mathbf{n} = -e_i \end{cases}$$

where  $e_j^{(i)} = \delta_{ij}$  denotes the  $i$ -th unit vector. In order to comply with the centralization property of  $Q$ -matrices, it follows that:

$$Q(\mathbf{n}, \mathbf{n}) = - \sum_{i=1}^N n_i(t)(1 - 2f_i(\mathbf{n}(t))) + f_i(\mathbf{n}(t)).$$

The analytical gain function  $f_i(\mathbf{n}(t))$  defines the state transition rate of a unit  $i$ , given the state of the network,  $\mathbf{n}(t)$ , and it is assumed to take values in the range  $[0, 1]$ . Typically, this function is written as  $f_i(u_i(t))$ , where  $u_i(t)$ , which represents the input to the unit  $i$  with the scaling parameter  $0 < \gamma \leq 1$ , is written as

$$u_i(t) := \bar{J}K_i^{-\gamma} \sum_{j=1}^N J_{ij}n_j(t) + K_i^\gamma \mu_{0,i} \quad (1)$$

where  $\bar{J}$ ,  $K_i$ , and  $\mu_{0,i}$  are the coupling strength, the number of input units and the external drive to the  $i$ -th unit, respectively. For the convenience of the current presentation, we consider here networks with  $K_i = K$ ,  $f_i = f$  and  $\mu_{0,i} = \mu_0$  for all  $i$ . We will provide below (in eqns. 10 and 11) conditions on the network structure,  $\mathbf{J}$ , that imply the convergence of the averaged population activity in the network towards a deterministic limit

$$m(t) \stackrel{!}{=} \lim_{N \rightarrow \infty} \frac{1}{N} \sum_{i=1}^N n_i(t). \quad (2)$$

Here,  $m(t)$  is known as the mean-field limit and has the following temporal dynamics:

$$\frac{d}{dt}m(t) = -m(t) + F(m(t)) \quad (3)$$

for some a priori unknown function  $F$ . In order to determine  $F$ , we use the following semimartingale decomposition, that specifies the difference between  $\bar{n}(t) := \frac{1}{N} \sum_{i=1}^N n_i(t)$  (i.e., the average population activity of a finite-size net-

work) and the mean-field limit  $m(t)$  of the system,

$$\begin{aligned}\bar{n}(t) - m(t) &= (\bar{n}(0) - m(0)) - \int_0^t ds (\bar{n}(s) - m(s)) \\ &\quad + \int_0^t ds \left( \frac{1}{N} \sum_{i=1}^N f(u_i(t)) - F(m(s)) \right) \\ &\quad + \mathcal{M}(t),\end{aligned}\tag{4}$$

where  $\mathcal{M}(t)$  is some square integrable martingale that, according to the general theory of Markov processes [17], satisfies

$$\mathbb{E} [\mathcal{M}(t)^2] = \frac{1}{N^2} \int_0^t ds -Q(\mathbf{n}(s), \mathbf{n}(s)) \leq \frac{t}{N}.\tag{5}$$

Note that  $\mathbb{E}[\mathcal{M}(t)] = 0$  and, in general,  $\mathcal{M}(t)$  specify finite-size fluctuations in the average population activity. Provided that  $m(t)$  exists (refer to eqns. 10 and 11 for a justification of this ansatz), we can construct the function  $F$  by expanding  $\frac{1}{N} \sum_{i=1}^N f(u_i(t))$  as  $N \rightarrow \infty$  in eqn. 4 around

$$\mu_1(t) := K^{1-\gamma} \bar{J} m(t) + K^\gamma \mu_0.\tag{6}$$

Using the lemma that is described later in the Materials and Methods section, we obtain the following series expansion

$$F(m(t)) = f(\mu_1(t)) + \sum_{r=2}^{\infty} \frac{f^{(r)}(\mu_1(t))}{r!} \mu_r(t).\tag{7}$$

where  $\mu_1$  represents the average input to a unit in the network at time  $t$ . The higher order coefficients can be computed by expanding  $\mu_r := \lim_{N \rightarrow \infty} \frac{1}{N} \sum_{i=1}^N [(u_i - \mu_1)^r]$ . The second order coefficient is given by:

$$\mu_2(t) = \bar{J}^2 K^{1-2\gamma} m(t)(1 - m(t))\tag{8}$$

and the subsequent coefficients are given by:

$$\mu_r(t) = \bar{J}^r K^{-r\gamma} \sum_{q=0}^r a_q m(t)^q \sum_{s=0}^{r-q} b_s m(t)^s\tag{9}$$

where,

$$a_q := \binom{r}{q} (-1)^q K^q$$

and

$$b_s := \mathcal{S}(r - q, s)(K)_s$$

Here,  $\mathcal{S}$  is a Stirling number of the second kind and  $(\cdot)_s$  denotes the falling factorial. In the binomial expansion of  $\mu_r(t)$  given in eqn. 9, the summation

over  $j$  is performed using the ansatz that  $m(t)$  exists; thereafter, summation over  $i$  in the average operator  $\lim_{N \rightarrow \infty} \frac{1}{N} \sum_{i=1}^N [\cdot]$  is applied. In order to provide the necessary conditions for the existence of a deterministic limit,  $m(t)$ , the summation order must be changed. Therefore, the first condition for  $m(t)$  and  $\mu_1(t)$  to exist is

$$\lim_{N \rightarrow \infty} \frac{1}{N} \sum_{j=1}^N \left[ \sum_{i=1}^N J_{ij} - K \right] = 0. \quad (10)$$

Eqn. 10 implies that the coefficient in front of  $f'$  in the series expansion that leads to eqn. 7 vanishes in the thermodynamic limit (refer to the Materials and Methods section for a detailed description). The second condition for the pointwise convergence of an averaged population activity to the mean-field limit in eqn. 2 is given by

$$\lim_{N \rightarrow \infty} \frac{1}{N} \sum_{j_1 \neq j_2}^N \left[ \sum_{i=1}^N J_{ij_1} J_{ij_2} - K(K-1) \right] = 0. \quad (11)$$

This condition specifies that, as  $N \rightarrow \infty$ , the mean covariance of columns in the connectivity matrix  $\mathbf{J}$  must decay to zero. The higher order condition can be similarly determined in order to achieve a pointwise convergence of the averaged population activity to its mean-field limit, as described in eqn. 3 (refer to the Materials and Methods section for calculation details).

It is often of interest to study network dynamics when the number of inputs into units is large (e.g.  $K \rightarrow \infty$ ). In order to study this classical case, we must investigate the asymptotic behavior of  $\mu_r$  in eqn. 9 in the order of  $K$ ; it can be observed that the odd coefficients are given by

$$\mu_{2k+1} \sim \mathcal{O}(K^{1-(2k+1)\gamma})$$

and the even coefficients are given by

$$\mu_{2k} \sim \mathcal{O}(K^{1-2k\gamma}) + (2k)!! \mu_2^k,$$

for  $k \in \mathbb{N}$ . Hence, it is apparent that the scaling parameter  $\gamma$  plays a critical role in the large  $K$  limit. In classical balanced-state theory [18], the scaling parameter  $\gamma$  is generally assumed to take the value 0.5; in this case,  $\mu_2 \sim \mathcal{O}(1)$  and the mean-field coefficients of eqn. 3 converge as  $K \rightarrow \infty$ , towards the central moments of a Gaussian distribution function. As a result, the related power series that is given by eqn. 7 can be reformulated in terms of a simple Gaussian integral so that, in this special case, eqn. 3 reduces to

$$\frac{d}{dt} m(t) = -m(t) + \int dx \frac{f(x)}{\sqrt{2\pi\mu_2(t)}} \exp\left(-\frac{(x - \mu_1(t))^2}{2\mu_2(t)}\right). \quad (12)$$

In the above analysis, we first take  $N \rightarrow \infty$  to arrive at the mean-field of eqn. 3 and then we consider  $K \rightarrow \infty$  in order to recover eqn. 12. This derivation

generalizes the proposed limit ( $K \rightarrow \infty$ ) in eqn. A.7 of van Vreeswijk and Sompolinsky’s seminal work [18]. It is noteworthy that the analysis here shows that the finite  $K$  correction to eqn. 12 is relatively small for a homogeneous network; this is consistent with the approximation that is made in section 4.2 of [18].

The semimartingale decomposition that is given in eqn. 4 provides additional information on the expansion of networks that have finite size  $N$ . Using eqn. 5, we can determine the fluctuations magnitude of the average population activity in finite networks in the mean-square sense as

$$\mathbb{E}(\mathcal{M}(t)^2) = \frac{1}{N^2} \int ds \sum_{i=1}^N (n_i(s)(1 - 2f(u_i(s))) + f(u_i(s))).$$

and, by expanding  $\frac{1}{N} \sum_{i=1}^N f(u_i(t))$  at  $\mu_1(t)$ , we arrive at

$$\mathbb{E}(\mathcal{M}(t)^2) = \frac{1}{N} \int_0^t ds (m(s)(1 - 2(g(\mu_1) + \mathcal{R})) + g(\mu_1) + \mathcal{R})$$

where  $g(\mu_1) := f(\mu_1(t)) + f''(\mu_1)\mu_2/2$  and  $\mathcal{R} := \sum_{r=3}^{\infty} \frac{f^{(r)}(\mu_1)}{r!} \mu_r$  denotes the remainder terms of the expansion. The average population activity dynamics of a finite size network can be described approximately in terms of the following Ornstein-Uhlenbeck process

$$d\bar{n}(t) \approx (-m(t) + F(m(t)))dt + \frac{\sigma(t)}{\sqrt{N}}d\mathcal{B}_t \quad (13)$$

where  $\sigma^2(t) := m(t)(1 - 2g(\mu_1(t)) + g(\mu_1(t)))$  and  $\mathcal{B}$  is Brownian motion. In the approximation of eqn. 13, we ignore the contribution of remainder terms (e.g.,  $\mathcal{R}$ ) to  $\sigma(t)$ . It now becomes clear, that the fluctuating term of eqn. 13 vanishes in the thermodynamic limit.

### 3 Convergence to MFT in networks of binary neurons

In order to illustrate our complete MFT, we consider two scenarios that are relevant to the theoretical analysis of neural systems. The first scenario is that of a population network with a constant external input  $\mu_0 > 0$ . When  $\bar{J} < 0$  this system is the classical balanced network for which the external input is canceled by internal fluctuations. We choose a widely-used gain function in neural networks theory which it is given by

$$f(x) := \frac{1 + \text{Erf}(\alpha x)}{2}. \quad (14)$$

The parameter  $\alpha$  describes the intrinsic noise intensity of the individual units and therefore must be positive. When  $\alpha \rightarrow \infty$ , this transfer function approximates to the well-studied Heaviside step function [18]. Using the transfer function given by eqn. 15 (with  $\alpha = 5$ ) and a directed fixed-in-degree Erdős-Rényi

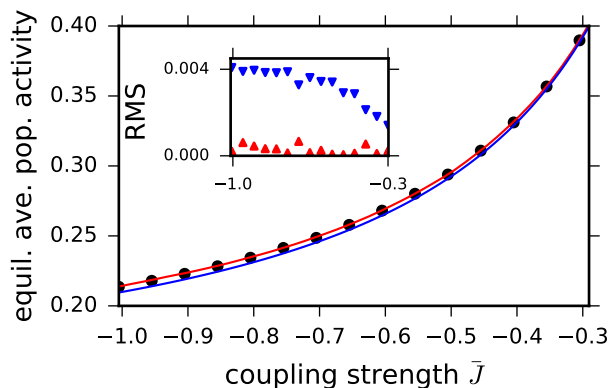


Figure 1: Convergence of the average population activity to the steady-state MFT predictions. The **red line** indicates the predictions of complete MFT in eqn. 3 and is computed as described in the Materials and Methods section. The **blue line** is the predictions of mean-field eqn. 12, assuming only Gaussian fluctuations. The **black dots** represent simulations of a network with  $N = 1000$  units averaged over 20 independent trails (error bars are smaller than symbol size). The **inset** is the root mean square of error between simulations and the complete theory (**upward red triangles**) and the Gaussian approximate theory (**downward blue triangles**). The simulations were performed using a Doob-Gillespie algorithm for  $T = 5 \times 10^5$  steps with the gain function given by eqn. 15. The averaged activity was estimated in the last  $5 \times 10^3$  steps across all trials. Parameters:  $\gamma = 0.5$ ,  $\alpha = 5$ ,  $K = 10$  and  $\mu_0 = 0.1$ .

network (with  $K = 10$ ), we compute the complete steady-state mean-field limit of eqn. 3, using the approximation described in the Materials and Methods section (Fig.1, red line). We compare the complete mean-field theory (Fig.1, red line) with the mean-field prediction that assumes only Gaussian statistics (i.e.,  $K \rightarrow \infty$ ) in eqn. 12 (Fig.1, blue line). The difference between the predictions becomes apparent as  $|\bar{J}|$  increases. Numerical simulations of a finite-size network ( $N = 1000$ ) are used to estimate the steady-state population activity by averaging 20 independent trials (Fig.1, black dots). The equilibrium population average activity of simulated networks (Fig.1, black dots) exhibits excellent agreement with both the complete (Fig.1, red line) and the Gaussian approximation (Fig.1, blue line) of the mean-field limit in the case of weak coupling. However, in cases where the coupling is strong, the average population equilibrium activity deviates from the Gaussian approximation (Fig.1, blue line) and, instead, follows the predictions of the complete mean-field limit (Fig.1, red line). Therefore, the Gaussian approximation that is given in eqn. 12 is only reasonable for weak coupling and relatively large value of  $K$ . The error between steady-state population activity from the simulations (Fig.1, black dots) and the Gaussian approximation (Fig.1, blue line) increases as  $|\bar{J}|$  becomes larger (Fig.1, downward blue triangles in the inset). However, the error between averaged activity of the simulated networks and the complete MFT stays almost constant (Fig.1, upward red triangles in the inset); this error is due to the truncation of the series expansion and the numerical stability of power-series representation underlies the function  $F$  in eqn. 7 (refer to Materials and Methods section for more details).

In order to illustrate our complete MFT, we consider two scenarios that are relevant to the theoretical analysis of neural systems. The first scenario is that of a population network with a constant external input  $\mu_0 > 0$ . When  $\bar{J} < 0$  this system is the classical balanced network for which the external input is canceled by internal fluctuations. We choose a widely-used gain function in neural networks theory which it is given by

$$f(x) := \frac{1 + \text{Erf}(\alpha x)}{2}. \quad (15)$$

The parameter  $\alpha$  describes the intrinsic noise intensity of the individual units and therefore must be positive. When  $\alpha \rightarrow \infty$ , this transfer function approximates to the well-studied Heaviside step function [18]. Using the transfer function given by eqn. 15 (with  $\alpha = 5$ ) and a directed fixed-in-degree Erdős-Rényi network (with  $K = 10$ ), we compute the complete steady-state mean-field limit of eqn. 3, using the approximation described in the Materials and Methods section (Fig.1, red line). We compare the complete mean-field theory (Fig.1, red line) with the mean-field prediction that assumes only Gaussian statistics (i.e.,  $K \rightarrow \infty$ ) in eqn. 12 (Fig.1, blue line). The difference between the predictions becomes apparent as  $|\bar{J}|$  increases. Numerical simulations of a finite-size network ( $N = 1000$ ) are used to estimate the steady-state population activity by averaging 20 independent trials (Fig.1, black dots). The equilibrium population average activity of simulated networks (Fig.1, black dots) exhibits excellent



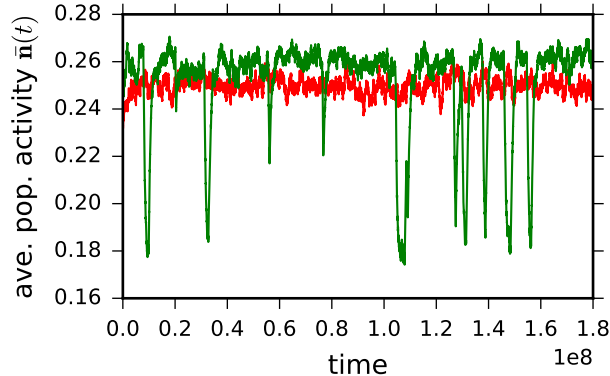


Figure 2: Emergence of stochastic MFT. The **green line** shows the temporal evolution of a simulated network with  $N = 5000$  and  $K = 10$ ; this network does not have a deterministic MFT since the condition in eqn. 10 is not satisfied. The out-degree of a single unit in the network was set to be  $N$  (i.e.,  $\rho = 1$  in eqn. 16). For comparison, the **red line** shows the average population activity of a similar network for which  $\rho = K/N$ . The system time in x-axis is calculated according to a Doob-Gillespie algorithm (the average update interval is  $dt = 1368.6$ , refer to the Materials and Methods section for details). Parameters:  $\bar{J} = -0.7$  and all other parameters are as in Fig.1.

agreement with both the complete (Fig.1, red line) and the Gaussian approximation (Fig.1, blue line) of the mean-field limit in the case of weak coupling. However, in cases where the coupling is strong, the average population equilibrium activity deviates from the Gaussian approximation (Fig.1, blue line) and, instead, follows the predictions of the complete mean-field limit (Fig.1, red line). Therefore, the Gaussian approximation that is given in eqn. 12 is only reasonable for weak coupling and relatively large value of  $K$ . The error between steady-state population activity from the simulations (Fig.1, black dots) and the Gaussian approximation (Fig.1, blue line) increases as  $|\bar{J}|$  becomes larger (Fig.1, downward blue triangles in the inset). However, the error between averaged activity of the simulated networks and the complete MFT stays almost constant (Fig.1, upward red triangles in the inset); this error is due to the truncation of the series expansion and the numerical stability of power-series representation underlies the function  $F$  in eqn. 7 (refer to Materials and Methods section for more details).

The hierarchy of conditions on the connectivity matrix  $\mathbf{J}$  (eqns. 10 and 11) guarantees the convergence of the average population activity to the prediction of MFT. In particular, eqn. 10 indicates that, as  $N \rightarrow \infty$ , the average column sum of the connectivity matrix  $\mathbf{J}$  should be  $K$ . It is straightforward to construct networks that do not obey this rule; such networks lose their pointwise convergence to a deterministic mean-field limit in eqn. 3. An extreme example

of a network of this kind is a network that has a single unit,  $n_{j_*}$ , that connects into  $\rho N$  neurons in the circuits, where  $0 < \rho \leq 1$  is the fraction of units in the network that are post-synaptic for  $n_{j_*}$ . Numerical simulations of such a network ( $N = 5000$  and  $\rho = 1$ ) show large-amplitude population activity fluctuations (Fig.2, green line), in contrast to the smaller fluctuations of a homogeneous network (Fig.2, red line). Our approach allows the construction of stochastic correction terms to the mean-field limit by isolating the unit  $n_{j_*}$  from the network and then taking the limit  $N \rightarrow \infty$ . Therefore, a first-order correction to the function  $F$  of eqn. 7 can be derived as

$$F_s(m(t)) \approx F(m(t)) + \rho \bar{J} K^{-\gamma} f'(\mu_1(t)) n_{j_*}(t). \quad (16)$$

$F_s$  is a stochastic function since  $n_{j_*}$  is a binomial random variable for which the probability of being at state one is  $m(t)$ ; the mean-field equation is thus transformed into an ordinary stochastic differential equation. The correction term in eqn. 16 indicates that the observed large fluctuations (Fig.2, green line) are indeed a finite  $K$  phenomenon. Therefore, in large networks that have a finite number of connections between units (e.g. finite  $K$  networks), it suffices that only one unit breaks the condition (i.e.,  $\rho > 0$ ) and, as a result, the deterministic MFT collapses. The emergence of large-amplitude population events in Fig.2 has been observed previously as the indication of the ‘‘synfire chain’’ in cortical networks [2]. It is noteworthy that there is compelling evidence that such structures exist in cortical microcircuits [9] and recent experimental results indicate that the diverse couplings between single-cell activity and population averages [11] suggest the existence of this polychronous state [8] in cortical networks.

## 4 Discussion

In this paper, we considered a simple network of  $N$  binary units of which the recurrent interactions can be in balance with the excitatory feedforward input. This simplified model captures the essential aspects of cortical asynchronous state [18], and it allowed us to demonstrate, with extra clarity, the calculation of a complete MFT for finite-size systems dynamics with arbitrary connectivity structure. The model neurons are two-state units that update their state stochastically. The updated state of a single unit is either active with a probability given by  $f(\mathbf{n}(t))$  or in a state of quiescence. Our results show that the MFT for binary units is fundamentally constructed from the Law of Large Numbers (LLNs) and the emergence of intrinsic fluctuations does not require the application of the central limit theorem. We further demonstrate the dependence of averaged population activity fluctuations on both the system size,  $N$ , and the average number of connections per unit,  $K$ . Furthermore, our formalism allows the study of a finite-size network in the form of an ordinary stochastic differential equation (eqns. 13 and 16). Noteworthy, the method presented here relies on our ability to calculate the function  $F$  of eqn. 7. A more efficient representation for finite  $K$  networks, similar to the large  $K$  limit in eqn. 12, provides a further means to investigate systems with very strong coupling schemes.

Our approach in this paper goes beyond the classical asymptotic analysis of random connectivities, and the theory specifies a hierarchy of conditions that require a pointwise convergence to the deterministic mean-field limit. We show that a stochastic population spike emerges, irrespective of the network size, by breaking the first condition (eqn. 10). The activity of units in this state can be reproducibly time locked; however, the network state remains asynchronous. This dynamic state captures the important features that are required for polychronous activity, which produces precise time coding for cognitive computations [8]. Indeed, such polychronous activity may also correspond to the observation of unitary events [13, 2] or give rise to the diverse coupling of neurons to the population dynamics in the cortex [11].

Our results indicate a broad array of connectivity motifs for which network collective dynamics lie in lower dimensional space of the mean-field limit; individual units or sub-populations do not, therefore, alter the collective network behavior in the thermodynamic limit. Moreover, a hierarchy of conditions for the pointwise convergence to the deterministic limit illustrates the potential influence of inhomogeneous microstructures on aggregate network dynamics. Our approach provides a new perspective for the investigation of biologically realistic cortical computations and plasticity, thus going beyond the asynchronous-state analysis.

## 5 Materials and Methods

### 5.1 Calculation of the mean-field equation and sufficient conditions for its validity

The mean-field equation that is given by eqn. 3 is the direct result of the Taylor expansion of  $\frac{1}{N} \sum_{i=1}^N f(u_i(t))$ , and it appears in the drift term of eqn. 4, at  $\mu_1(t)$ , the presumed average input to each unit. Indeed, for an analytical  $f$ , we have

$$\begin{aligned} \frac{1}{N} \sum_{i=1}^N f(u_i(t)) &= f(\mu_1(t)) + f'(\mu_1(t)) \left( \frac{1}{N} \sum_{i=1}^N u_i(t) - \mu_1(t) \right) \\ &\quad + \sum_{r=2}^{\infty} \frac{f^{(r)}(\mu_1(t))}{r!} \frac{1}{N} \sum_{i=1}^N (u_i(t) - \mu_1(t))^r. \end{aligned}$$

Thus, it becomes apparent that, in the case of convergence  $\mu_1(t) = \lim_{N \rightarrow \infty} \frac{1}{N} \sum_{i=1}^N u_i(t)$ , in eqn. 7 the term corresponding to  $f'$  vanishes. Inserting the definition of  $u_i$  in eqn. 1 implies that the convergence is equivalent to

$$\lim_{N \rightarrow \infty} \frac{1}{N} \sum_{i=1}^N \sum_{j=1}^N J_{ij} n_j(t) = Km(t). \quad (17)$$

Interchanging the summation and assuming the convergence  $m(t) = \lim_{N \rightarrow \infty} \frac{1}{N} \sum_{i=1}^N n_i(t)$ , which is equivalent to

$$\lim_{N \rightarrow \infty} \frac{1}{N} \sum_{j=1}^N \left( \sum_{i=1}^N J_{ij} - K \right) n_j(t) = 0. \quad (18)$$

Next observe that the conditional distribution of  $(n_j(t))$  on a typical realization of  $(J_{ij})$  is exchangeable. This implies in particular, using the notation  $\bar{J}_{ij} := J_{ij} - \frac{K}{N}$ , that

$$\begin{aligned} & \mathbb{E} \left( \left( \frac{1}{N} \sum_{j=1}^N \sum_{i=1}^N \bar{J}_{ij} n_j(t) \right)^2 \right) \\ &= \frac{1}{N^2} \sum_{j_1, j_2=1}^N \mathbb{E} \left( \sum_{i=1}^N \bar{J}_{ij_1} \sum_{i=1}^N \bar{J}_{ij_2} \mathbb{E}(n_{j_1}(t) n_{j_2}(t) \mid (J_{ij})) \right) \\ &= \frac{1}{N^2} \sum_{j_1=j_2=1}^N \mathbb{E} \left( \left( \sum_{i=1}^N \bar{J}_{ij_1} \right)^2 \mathbb{E}(n_1(t) \mid (J_{ij})) \right) \\ &\quad + \frac{1}{N^2} \sum_{j_1 \neq j_2=1}^N \mathbb{E} \left( \sum_{i=1}^N \bar{J}_{ij_1} \sum_{i=1}^N \bar{J}_{ij_2} \mathbb{E}(n_{j_1}(t) n_{j_2}(t) \mid (J_{ij})) \right) \\ &= \frac{1}{N^2} \sum_{j=1}^N \mathbb{E} \left( \left( \sum_{i=1}^N \bar{J}_{ij} \right)^2 \mathbb{E}(n_{j_1}(t)(1 - n_{j_2}(t)) \mid (J_{ij})) \right) \\ &\quad + \mathbb{E} \left( \left( \frac{1}{N} \sum_{j=1}^N \sum_{i=1}^N \bar{J}_{ij} \right)^2 \mathbb{E}(n_{j_1}(t) n_{j_2}(t) \mid (J_{ij})) \right). \end{aligned}$$

Hence convergence in eqn. 18 holds, provided

$$\frac{1}{N} \sum_{j=1}^N \left[ \sum_{i=1}^N J_{ij} - K \right] \rightarrow 0$$

as  $N \rightarrow \infty$ . This condition essentially is the weak LLNs for the column sum of the connectivity matrix of the network. The second condition in eqn. 11 can also be computed by the binomial expansion of

$$\lim_{N \rightarrow \infty} \frac{1}{N} \sum_{i=1}^N \left[ \left( \bar{J} K^{-\gamma} \sum_{j=1}^N J_{ij} n_j(t) - K^{1-\gamma} \bar{J} m(t) \right)^2 \right].$$

By exchanging the summations order, we seek to determine a condition for this to equate  $\mu_2$  in eqn. 8. Thus, provided that eqn. 10 holds, we must additionally

satisfy the condition that

$$\lim_{N \rightarrow \infty} \frac{1}{N} \left[ \sum_{j_1 \neq j_2 = 1}^N \sum_{i=1}^N J_{ij_1} J_{ij_2} - K(K-1) \right] = 0.$$

Hence, the condition can be simplified to that described by eqn. 11 and we can recover  $\mu_2$ . The subsequent  $r$ -th order condition can be similarly derived to construct function  $F$  in eqns. 7 and 4 by expanding

$$\lim_{N \rightarrow \infty} \frac{1}{N} \sum_{i=1}^N \left[ (\bar{J} K^{-\gamma} \sum_{j=1}^N J_{ij} n_j(t) - K^{1-\gamma} \bar{J} m(t))^r \right].$$

More specifically, we need that

$$\lim_{N \rightarrow \infty} \frac{1}{N} \left[ \sum_{j_1 \neq j_2 \neq \dots \neq j_r = 1}^N \sum_{i=1}^N J_{ij_1} J_{ij_2} \dots J_{ij_r} - (K)_r \right] = 0.$$

## 5.2 Numerical computation of the mean-field limit

Power series computation is, in general, difficult; the power series in eqn. 7 has weak convergence for large values of  $\bar{J}$ . Here, we transform the power series in eqn. 7 into a computationally more efficient representation. First, we derive a close form for the coefficients of eqn. 9 by using the identity that  $(K)_s = s! \binom{K}{s}$ , thus

$$\mu_r = \bar{J}^r K^{-r\gamma} \sum_{q=0}^r \binom{r}{q} (-1)^q K^q m^q \sum_{s=0}^w \mathcal{S}(w, s) s! \binom{K}{s} m^s$$

where  $w := r - q$ . The second sum is the  $w$ -th moment of the binomial random variable

$$\Delta^{(w)} := \sum_{s=0}^w \mathcal{S}(w, s) s! \binom{K}{s} m^s = \left( \frac{d^w}{dt^w} (1 - m + me^t)^K \right) \Big|_{t=0}.$$

Hence,

$$\mu_r = \bar{J}^r K^{-r\gamma} \sum_{q=0}^r \binom{r}{q} (-1)^q K^q m^q \Delta^{(w)}.$$

$\Delta^{(w)}$  admits the following representation

$$\Delta^{(w)} = (Km)^w + a_{w-1} (Km)^{w-1} + \dots + a_0$$

as a polynomial in the variable  $Km$  of degree  $w$  with leading coefficient 1. For large  $K$  the approximation  $\Delta^{(w)} \sim (Km)^w$  therefore leads to the following approximation of eqn. 9

$$\mu_r \approx \bar{J}^r K^{r-r\gamma} m^r \sum_{q=0}^r \binom{r}{q} (-1)^q$$

and using

$$\sum_{q=0}^r \binom{r}{q} (-1)^q = \frac{(-1)^r (2 - 2^{-r})}{2} + \frac{{}_2\mathcal{F}_1(1, 1, 1 - r, -1) \sin(\pi r)}{\pi r}$$

where  ${}_2\mathcal{F}_1$  is a hypergeometric function [1], we arrive at the following approximation

$$\mu_r \approx \bar{J}^r K^{r-r\gamma} m^r \left( \frac{(-1)^r (2 - 2^{-r})}{2} + \frac{{}_2\mathcal{F}_1(1, 1, 1 - r, -1) \sin(\pi r)}{\pi r} \right).$$

By inclusion of the second order and drift terms of the polynomial representation of  $\Delta^{(w)}$  in the series, one can improve the approximation

$$\begin{aligned} \mu_r \approx & \bar{J}^r K^{-r\gamma} ((1 + Km)^{-1-r} (1 + 2Km + K^2(-1 + m)m) \\ & \left( -(-Km)^r + (-Km(1 + Km))^r + \right. \\ & \left. Km(-Km(1 + Km))^r + \frac{{}_2\mathcal{F}_1(-r, -r, 1 - r, -Km) \sin(\pi r)}{\pi r} \right) \end{aligned}$$

The inclusion of more terms in the expansion of  $\Delta^{(w)}$  in the series allows one to determine an arbitrarily precise value for  $\mu_r$ . For the particular gain function  $f$  in eqn. 15 the resulting function  $F$  in eqn. 7 can be efficiently evaluated numerically for small  $\bar{J}$  using the following representation

$$f^{(r)}(x) = \frac{(-1)^{r-1}}{\sqrt{\pi}} H_{r-1}(x) e^{-x^2}$$

for its higher order derivatives. Here,  $H_r$  is the  $r$ -th order Hermite polynomial. In Fig.1, we computed the series expansion

$$F(m; v) := f(\mu_1) + \sum_{r=2}^v \frac{f^{(r)}(\mu_1)}{r!} \mu_r$$

up to a summation index  $v$  satisfying  $F(m; v) \sim F(m; v - 1)$  with the above approximation of  $\mu_r$  to evaluate the complete mean-field limit (Fig.1, red line). Note that this numerical approximation requires the smallness of  $\bar{J}K^{-\gamma}$ .

### 5.3 Simulation of the binary networks

In order to simulate the binary networks, we use an exact stochastic simulation of interactions in the network using the  $Q$ -matrix of Markovian dynamics. The simulations follow the standard Doob-Gillespie algorithm [3, 4]. In brief, given the state  $(n_i(t))$  at time  $t$ , the waiting time  $\tau$  until the next update at time  $t + \tau$  is exponentially distributed with rate  $\sum_{i=1}^N \phi_i(t)$ , where

$$\phi_i(t) := (1 - n_i(t))f(u_i(t)) + n_i(t)(1 - f(n_i(t))).$$

The updated unit  $i_*$  is chosen according to the distribution  $\phi_i(t) / \sum_{i=1}^N \phi_i(t)$ , and its state is switched (i.e.  $n_{i_*}(t) \mapsto 1 - n_{i_*}(t)$ ).

## 5.4 Derivation of stochastic mean-field limit

In order to derive the approximation of the stochastic mean-field limit in eqn.16, we rewrite the coefficient of  $f'$  using condition 18. We isolate unit  $n_{j_*}$  with  $\rho N$  post-synaptic coupling and sum the rest of the network. Construction of the rest of the network satisfies eqn. 10 and the coefficient related to the stochastic state transition of unit  $n_{j_*}$  remains as  $N \rightarrow \infty$ .

## Acknowledgement

We thank Viktor Ørduuk Sandberg, Carl van Vreeswijk and Rainer Engelken for invaluable and critical feedback. This work was supported by the the Federal Ministry of Education and Research (BMBF) Germany under Grant no. FKZ01GQ1001B.

## References

- [1] M. Abramowitz and I. A. Stegun. *Handbook of Mathematical Functions: with Formulas, Graphs, and Mathematical Tables*. Dover Publications, June 1965.
- [2] Y. Aviel, C. Mehring, M. Abeles, and D. Horn. On embedding synfire chains in a balanced network. *Neural computation*, 15(6):1321–1340, 2003.
- [3] J. L. Doob. Topics in the theory of Markoff chains. *Transactions of the American Mathematical Society*, 52(1):37–64, 1942.
- [4] D. T. Gillespie. A general method for numerically simulating the stochastic time evolution of coupled chemical reactions. *Journal of Computational Physics*, 22(4):403–434, Dec. 1976.
- [5] R. J. Glauber. Time-dependent statistics of the ising model. *Journal of Mathematical Physics*, 4(2):294–307, Feb. 1963.
- [6] M. Helias, T. Tetzlaff, and M. Diesmann. The Correlation Structure of Local Neuronal Networks Intrinsically Results from Recurrent Dynamics. *PLoS Comput Biol*, 10(1):e1003428, Jan. 2014.
- [7] S. L. Hill, Y. Wang, I. Riachi, F. Schürmann, and H. Markram. Statistical connectivity provides a sufficient foundation for specific functional connectivity in neocortical neural microcircuits. *Proceedings of the National Academy of Sciences*, 109(42):E2885–E2894, Oct. 2012.
- [8] E. M. Izhikevich. Polychronization: computation with spikes. *Neural computation*, 18(2), 2006.
- [9] W.-C. A. Lee, V. Bonin, M. Reed, B. J. Graham, G. Hood, K. Glattfelder, and R. C. Reid. Anatomy and function of an excitatory network in the visual cortex. *Nature*, 532(7599):370–374, Apr. 2016.

- [10] A. Luczak, P. Barthó, S. L. Marguet, G. Buzsáki, and K. D. Harris. Sequential structure of neocortical spontaneous activity in vivo. *Proceedings of the National Academy of Sciences*, 104(1):347–352, Jan. 2007.
- [11] M. Okun, N. A. Steinmetz, L. Cossell, M. F. Iacaruso, H. Ko, P. Barthó, T. Moore, S. B. Hofer, T. D. Mrsic-Flogel, M. Carandini, and K. D. Harris. Diverse coupling of neurons to populations in sensory cortex. *Nature*, 521(7553):511–515, May 2015.
- [12] A. Renart, J. d. l. Rocha, P. Bartho, L. Hollender, N. Parga, A. Reyes, and K. D. Harris. The Asynchronous State in Cortical Circuits. *Science*, 327(5965):587–590, Jan. 2010.
- [13] A. Riehle, S. Grün, M. Diesmann, and A. Aertsen. Spike Synchronization and Rate Modulation Differentially Involved in Motor Cortical Function. *Science*, 278(5345):1950–1953, Dec. 1997.
- [14] M. N. Shadlen and W. T. Newsome. The Variable Discharge of Cortical Neurons: Implications for Connectivity, Computation, and Information Coding. *The Journal of Neuroscience*, 18(10):3870–3896, May 1998.
- [15] S. Song, P. J. Sjöström, M. Reigl, S. Nelson, and D. B. Chklovskii. Highly Nonrandom Features of Synaptic Connectivity in Local Cortical Circuits. *PLoS Biology*, 3(3):e68, 2005.
- [16] C. F. Stevens and A. M. Zador. Input synchrony and the irregular firing of cortical neurons. *Nature Neuroscience*, 1(3):210–217, July 1998.
- [17] D. W. Stroock. *An Introduction to Markov Processes*. Springer, Berlin; New York, 2005 edition, Oct. 2008.
- [18] C. van Vreeswijk and H. Sompolinsky. Chaotic balanced state in a model of cortical circuits. *Neural Comput*, 10(6):1321–71, Aug. 1998.